Flux Calibration of the Radio Telescope Esteban Bajaja from the Instituto Argentino de Radioastronomía

S.B. Araujo Furlan[1,2], G. Gancio[1], C.A. Galante[1,2] & G.E. Romero[1,2]

[1] *Instituto Argentino de Radioastronomía, CONICET–CICPBA–UNLP, Argentina*
[2] *Facultad de Matemática, Astronomía, Física y Computación, UNC, Argentina*
[3] *Facultad de Ciencias Astronómicas y Geofísicas, UNLP, Argentina*

Contact / saraujo@iar.unlp.edu.ar

Resumen / Presentamos el estado actual del trabajo de calibración en flujo del radiotelescopio Esteban Bajaja, de 30 m de diámetro, del Instituto Argentino de Radioastronomía (IAR). Para la calibración realizamos observaciones de una fuente de ruido interna (MC7014 ENR 35dB) y de fuentes astronómicas calibradoras de flujo conocido, como Fornax A. Las observaciones de las fuentes consistieron en barridos en ascensión recta y en declinación, de las cuales se registró la potencia en ambas polarizaciones lineales del radiotelescopio. De manera intercalada a cada barrido, se tomaron mediciones de la potencia asociada a la fuente de ruido. En el receptor empleamos una placa ROACH, en reemplazo de las placas ETTUS que se empleaban previamente. La frecuencia central de las observaciones fue de 1420 MHz, con un ancho de banda de 400 MHz, usando el máximo tiempo de integración, 600 ms.

Abstract / We present the current status of the flux calibration of the Radio Telescope Esteban Bajaja from the *Instituto Argentino de Radioastronomía* (IAR). We made observations of a noise source (MC7014 ENR 35dB) and of well-known astronomical sources, such as Fornax A. The observations consisted of scans on right ascension and declination, centred at the position of the sources. During each scan, the power of both linear polarization signals was registered, switching between the astronomical source and the noise source. We made the observations using the new receiver with a ROACH board, which replaces the old ETTUS boards. The central frequency was 1420 MHz, with a total bandwidth of 400 MHz and a maximum integration time of 600 ms.

Keywords / instrumentation: detectors — methods: observational — methods: data analysis — radio continuum: general

1. Introduction

When taking measurements from a telescope, one fundamental step necessary to obtain a valid result is the process of flux calibration. Through this process, we ensure that the results are comparable to those of other telescopes and even that measurements made with the same telescope at different times are consistent.

With the ongoing updates that take place in the receivers of the radio telescopes at the Instituto Argentino de Radioastronomía (IAR)(Gancio et al., 2020), it became essential to perform a new calibration of the system. One of the main upgrades implemented was the replacement of the digitizer ETTUS board with a more sensitive ROACH board.

To carry out the systematization of calibration measurements we followed the technique described in O´Neil (2002) and Marr et al. (2016): the Switched Noise Diode (SND) technique. This method resorts to measurements of the blank sky with the diode on and off. The diode available at the IAR is MC7014 ENR 35dB, plus several dimmers to reduce the total power injected. This method needs to know the effective temperature of the diode. Unfortunately, the datasheet of the diode does not specify the effective temperature at the observing frequency. To obtain it, we used for our calibration an astronomical source with known and non-variable flux density at radio frequencies (See Sect. 3.2).

In what follows we present the results of the analysis that we carried out to obtain the effective temperature of the noise diode.

2. The instrument

The instrument to be characterized is the Esteban Bajaja radiotelescope at the IAR. The signal obtained from the telescope goes into the digitalization module and splits in two directions: one to the old ETTUS board and one to the ROACH board, each one of them receiving exactly the same signal. That way, we can make different experiments while calibrating the ROACH board without affecting other ongoing observational campaigns.

The radio telescope has a diameter of 30 m and an angular resolution of 30′ at 1400 MHz. We observed in continuum mode, at a central frequency of 1420 MHz with a bandwidth of 400 MHz for each linear polarization. We chose a maximum integration time of 600 ms.

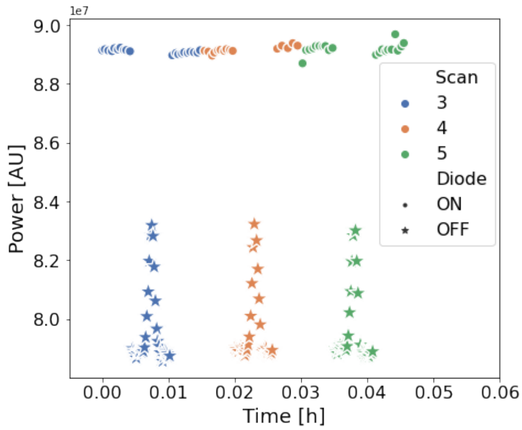

Figure 1: Three consecutive scans in declination for Fornax A on 07/13/22. The plot shows the power measured in arbitrary units vs. time in hours. Each scan is shown in a different colour, the circular markers correspond to observations with the diode on and the stars to observations with the diode off.

3. Methodology

3.1. Calibration procedure: switched observations

The SND method requires three different observations: 1) an observation of the blank sky with the diode on ($P_{\rm ON}$) to obtain the temperature associated with it ($T_{\rm cal}$), 2) one with the diode off ($P_{\rm OFF}$) to measure the system temperature ($T_{\rm off}$), and 3) an observation of the astronomical source ($P_{\rm source}$) to obtain the antenna temperature (T_A). T_A is related to the flux density of the source by:

$$T_A = \frac{1}{2}\frac{F_\nu\, A_{\rm eff}}{2\,k}, \quad (1)$$

where F_ν is the flux density of the astronomical source, $A_{\rm eff}$ is the effective area of the telescope and k is the Boltzmann constant. We divided the equation by 2 because we are considering only one of the two linear polarizations. In order to obtain $T_{\rm A}$, we follow the next relations:

$$T_{\rm A} = \frac{P_{\rm source} - P_{\rm OFF}}{P_{\rm OFF}}\, T_{\rm sys}, \quad (2)$$

$$T_{\rm sys} = \frac{P_{\rm OFF}}{P_{\rm ON} - P_{\rm OFF}}\, T_{\rm cal}, \quad (3)$$

where $P_{\rm OFF}$, $P_{\rm ON}$, and $P_{\rm source}$ are measurements of power in arbitrary units. In this case, we assume that the astronomical source is known and we want to obtain the temperature related to the diode ($T_{\rm cal}$) which is unknown.

3.2. Observational campaign

We observed five point-like sources with well-studied and non-variable flux densities at 1.42 GHz, taken from Testori et al. (2001): PKS 2152-69, PKS 0023-26, PKS 0131-36, PKS 0114-21 and PKS 0320-37. Here, we present the results of the calibration with Fornax A (PKS 0320-37). It is the brightest source observed, with a flux density of $F_{1.4\ \rm GHz} = 82.5$ Jy.

An observing session consisted of ten scans in declination and ten in right ascension, centered on the source and with a total length of 3.5° in each direction. At the beginning and at the end of the scans, we switched the diode on and kept the telescope in a fixed position. In Fig. 1 we show three consecutive scans for Fornax A. It can be seen that the power increases to a nearly constant value when the diode is on. The central part of the scan corresponds to the observation of the astronomical point source with the diode off. Fornax A was observed from 06/28/22 to 08/05/22. In the Section 4, we discuss the results for days 07/13/22 and 07/14/22.

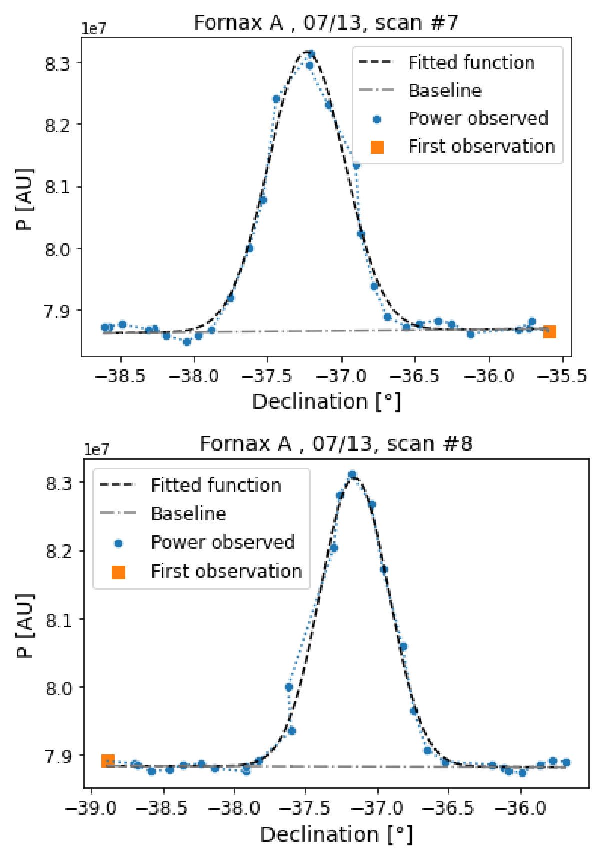

Figure 2: *Upper panel:* Power in arbitrary units (A.U.) for the scan in declination (N-S movement) of Fornax A. *Lower panel:* Power in arbitrary units (A.U.) for the scan in declination (S-N movement) of Fornax A. Both plots show the measurements taken, the fitted function, and the line fitting the baseline. The orange square indicates which observation was made first.

3.3. Data reduction

We adapted the software developed by Galante et al. (2022) to obtain the parameters given by Equations 2 and 3. We fitted each scan with a function consisting of the sum of a Gaussian and a linear function. The Gaussian modelled the emission from the astronomical source. The linear function modelled the power mea-

Scan	$(T_{\rm cal} \pm \Delta T_{cal})$ [K] 07/13/22	07/14/22
1	(7.0 ± 0.4)	(8.1 ± 0.5)
2	(7.0 ± 0.3)	(7.4 ± 0.5)
3	(7.5 ± 0.4)	(7.6 ± 0.4)
4	(7.4 ± 0.3)	(8.2 ± 0.4)
5	(7.5 ± 0.4)	(8.0 ± 0.4)
6	(7.5 ± 0.4)	(7.7 ± 0.4)
7	(7.2 ± 0.4)	(7.8 ± 0.5)
8	(7.7 ± 0.3)	(7.8 ± 0.5)
9	(7.7 ± 0.3)	(8.2 ± 0.5)
10	(8.0 ± 0.3)	(7.6 ± 0.6)
$\overline{T_{\rm cal}}$	(7.5 ± 0.4)	(7.8 ± 0.3)

Table 1: $T_{\rm cal}$ values with their respective error ΔT_{cal} obtained for each scan of Fornax A on the 07/13/22 and 07/14/22. The last row shows the mean value of all the scans for a day ($\overline{T_{\rm cal}}$).

sured while observing the blank sky with the diode off, i.e. the baseline. For scans in declination (δ), the function is given by

$$f(\delta) = P_{\rm peak} \, \exp\left(\frac{[-(\delta - \delta_0)]^2}{(2\,\sigma^2)}\right) + b\,\delta + c, \qquad (4)$$

where the power of the maximum is $P_{\rm peak}$, which is centered at δ_0; σ gives a measure of the width of the Gaussian, b is the slope of the baseline and c corresponds to its power offset.

First, using Eq. 1 we obtained $T_{\rm A}$ and used its value to get $T_{\rm sys}$ from Eq. 2, where we assigned each value of $P_{\rm peak}$ to the difference $P_{\rm source} - P_{\rm OFF}$. To get $P_{\rm OFF}$ we calculated the mean value of the points that were $3\,\sigma$ apart from δ_0. We could not use the fitted baseline for this because of the large errors in the adjusted parameters b and c. To obtain $P_{\rm ON}$ we computed the mean value of the points where the diode was on. Finally, we calculated $T_{\rm cal}$ from Eq. 3.

In this first analysis, we worked only with scans in declination. There is a difference between the speed at which the antenna moves while performing a scan and the speed at which the Earth rotates. This difference affects the shape of the scans in right ascension.

4. Results and analysis

On 07/13/22, the slope of the fitted baseline switched its sign depending if the antenna moved from South (S) to North (N) or vice-versa. In Fig. 2 we show the functions fitted and the corresponding baselines. To help distinguishing between N-S and S-N scans, we marked the first measured point with an orange square. This way we can see the difference between the slope of the baselines in both cases. This change in the slope could indicate a dependence of the antenna response in the direction in which it is moving. Another possibility is that the emission from the sky surrounding the astronomical source has an intrinsic slope. On 07/14/22, however, we did not detect the change in the slope of the baseline while observing the same source.

In Table 1 we present the obtained values of $T_{\rm cal}$ for each scan. In the last row, we show the mean value of $T_{\rm cal}$ for each day. Both mean values were similar within their errors. For 07/12/22 we obtained $\overline{T_{\rm cal}} = (7.5 \pm 0.4)$ and for 07/14/22 $\overline{T_{\rm cal}} = (7.8 \pm 0.3)$. However, we need to analyze a larger sample to verify this preliminary result. Besides Fornax A, the observations of the remaining sources were extremely noisy. Therefore, we were unable to use those observations to calculate the effective temperature of the diode at 1420 MHz.

5. Conclusion and future work

Being able to systematize the calibration process of the diode is necessary to get a reliable flux calibration for each observation made with the radio telescope. The use of a noise diode as a calibration source offers the advantage of not needing a nearby source of known and non-variable flux density at the time of the observation. A good flux calibration is essential to understand whether the possible variations are due to an external source or due to changes within the telescope and receiver, a crucial requirement in observations of variable sources such as blazars.

Following this remark, we observed a change in the slope of the baseline on a minute scale and also on a day-to-day basis. This traces a line of work in the future: identifying the source of the variability in the baseline. Being able to confirm the origin of the variation (external or internal) will help us to better characterize our instrument.

Regarding the systematization of the calibration process, we will finish adapting the script used in this work to add it to the automatic acquisition software of the antennas.

One way to check the obtained $T_{\rm cal}$ values is to look at other known non-variable sources and calculate their flux densities. This would be an indicator that our calibration process has been successful. As our observations of sources other than Fornax A were not usable, we were unable to perform this test.

To complete the diode calibration process, we plan to conduct another campaign, in order to obtain usable observations from several sources, to map the dependence of the antenna gain with the position on the sky, and to study the baseline variability.

References

Galante C.A., Romero G.E., Gancio G.A., 2022, BAAA, 63, 280

Gancio G., et al., 2020, A&A, 633, A84

Marr J.M., L. S.R., E. K.S., 2016, *Fundamentals of Radio Astronomy: Observational Methods*, Series in Astronomy and Astrophysics, CRC Press, Taylor & Francis Group

O´Neil K., 2002, *Single-Dish Calibration Techniques at Radio Wavelengths*, *Astronomical Society of the Pacific Conference Series*, vol. 278, 293–311

Testori J.C., et al., 2001, A&A, 368, 1123